

Assessment of the Reliability of Phased Array NDT of Coarse Grain Component Based on Simulation

Guillemette RIBAY¹, Steve MAHAUT, Gérard CATTIAUX³, Thierry SOLLIER³

¹ CEA Commissariat à l'Energie Atomique, Gif-sur-Yvette, France

² CEA LIST Centre de Saclay,

³ IRSN, Fontenay-aux-Roses, France

Contact e-mail: guillemette.ribay@cea.fr

Abstract. In this paper, we present the results of a study concerning the reliability of an ultrasonic phased array inspection dedicated to cast stainless steel used in nuclear power plants. This study was performed in the framework of a collaborative project between CEA and IRSN. The methodology of determination of Probability of Detection (POD), Probability of False Alarm (PFA) and Receiver Operating Characteristic (ROC) curves is presented. First, a detailed investigation of influent parameters was performed, using both NDT engineer knowledge and literature. Then a simplified approach was used to compute POD curves in coarse grain structures without increasing computation time. It is observed that fluctuations of the metallurgic structure of cast stainless steel are the most influent factors which degrade the reliability. Prior knowledge on stainless steel grade is also recommended. PFA were then obtained using experimental data. ROC curves were also deduced from PFA and POD for several defect sizes, which could help choosing an appropriate detection threshold depending on desired inspection capabilities.

Introduction

To ensure safety, components of a nuclear power plant have to be inspected on a regular basis to detect early damage. In particular, parts of the primary loop undergo severe conditions creating stress corrosion cracking initiated from the inner side of the metallic piping. Non-destructive techniques have been studied in the past to detect such defects. Among them, ultrasonic techniques are of particular interest as they do not require protection for the inspector. However, ultrasound may be strongly affected by the metallurgic structure of the component to inspect. This is especially encountered in centrifugally cast stainless steel (CCSS), where the size of the grains and the complex structure lead to attenuation of ultrasound and structural noise, making US inspection of cracks-like defects highly difficult. Moreover, the metallurgical structure may vary from one zone of the component to another, which makes it difficult to assess the detection capabilities of a given inspection procedure. In this paper, we focus on a new method of inspection of CCSS pipes by an ultrasonic phased array developed in a previous study. As part of a collaborative research project between CEA and IRSN, numerical tools based on CIVA software were used to assess the reliability of the method in terms of probability of detection (POD). In previous studies [1-3], model-based POD were used on other types of materials, mostly homogeneous ones; the present study focuses then on the problematic of model-based POD of heterogeneous materials like duplex stainless steel. After an investigation of the parameters likely to influence the outcome of an



inspection, POD curves were computed and the influence of some parameters is qualitatively determined, depending on the exact inspection procedure and application case. Lastly, Receiver-Operating-Characteristic curves are computed, using partly experiments and partly simulation tools.

1. Case Study

A new transducer dedicated to the inspection of CCSS components has been developed in a previous study [4], along with modelling tools in CIVA software that take into account the effect of the complex structure on ultrasound propagation and that were validated by experiment/simulation comparison in this previous study. The transducer central frequency is 500 kHz, and the transducer is made of two phased arrays mounted on a wedge and working in pitch-catch mode (figure 1). It is dedicated to the detection of bottom breaking notch that are normal to the bottom of the specimen; however, defects with other orientations close to normal could also be encountered, but the range of orientations was not available at the time of the study. Several CCSS components may be inspected by this method, with varying geometry that may not be precisely known; however, the component can be considered as locally cylindrical in shape, with a thickness varying from 75 to 90 mm. The objective of the study is then to show how the effect of coarse grain structure can be taken into account for model-based POD computation, and show how it can be used to help improve the inspection procedure if necessary. The component is inspected from the outside of the pipe, with longitudinal and circumferential scanning (figure 1). Delay laws are applied to the elements to enhance the detection of bottom breaking notch normal to the bottom specimen using longitudinal waves at 45° incidence.

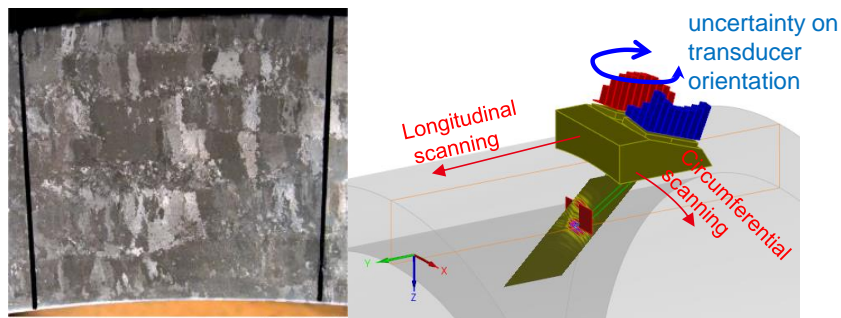


Fig. 1. Configuration of the case under study. Left, typical macrographic structure. Right, phased array on cylindrical component to inspect bottom breaking defect.

2. Analysis of Influent Parameters

The POD curves were all computed considering that the height of the defect is the characteristic parameter. The defect is modelled by a notch whose height varies from 5 to 30 mm, with a form factor of 2 between the height and the length of the notch. Prior to POD computation, parameters that may influence the signal amplitude were analysed. They are of several kinds:

- Parameters linked to the specimen itself (fluctuation of granular structure, geometry).
- Operating conditions: transducer positioning.
- Transducer characteristics.
- Defect characteristics.

The transducer characteristics are considered well-known (measurements are available to check them before the inspection).

As explained in the introduction, the metallurgic structure affects the propagation of ultrasound in two ways: first the measured signals may be noisy (creation of structural noise), and second the mean velocities and attenuation of the incident wave may be modified. The latter are modelled in CIVA using Born homogenization model: Indeed, the simulated medium will be considered as homogeneous with equivalent wave velocities and attenuation equal to the mean values at one inspection angle. Born model requires the knowledge of mean size of the metallurgical grains and of the elastic constants of the macro-grains (made of austenite). The mean grain size was determined with macrographs on representative mock-ups. Numerous macrographs were done on different parts of the pipe to retrieve the fluctuations of mean grain size inside the component. Automated image processing was applied to determine the mean grain size on each macrograph. The processing steps are given in figure 2. After adaptive equalization of the histogram and smoothing of the image, the image is segmented. Grain sizes are computed and averaged, excluding too small grains that do not have a significant effect on ultrasound. Depending on the zone of the mock-up, mean grain sizes ranging from 7.4 to 9.6 mm were found.

Elastic constant (c_{ij}) of mono-crystals of austenite had been previously measured on a sample of the mock-up [5]. However, to get information about the potential fluctuations of c_{ij} , several experiments would be necessary. Ledbetter et al.[6] gave a synthesis of c_{ij} measurement in various publications depending on the percentage of Chrome and Nickel in the stainless steel component. Assuming we do not know the grade of stainless steel composing our specimen, c_{ij} are known with significant uncertainty. Indeed, following these authors, c_{11} may range from 191.2 to 215.9 GPa, c_{12} from 118 to 145 GPa, and c_{44} from 123 to 138.6 GPa. However, knowing the stainless steel grade, the uncertainty is limited (c_{11} ranges from 200 to 207 GPa; c_{12} from 132 to 138 GPa; c_{44} from 123 to 132 GPa). Both situations will be considered in this paper.

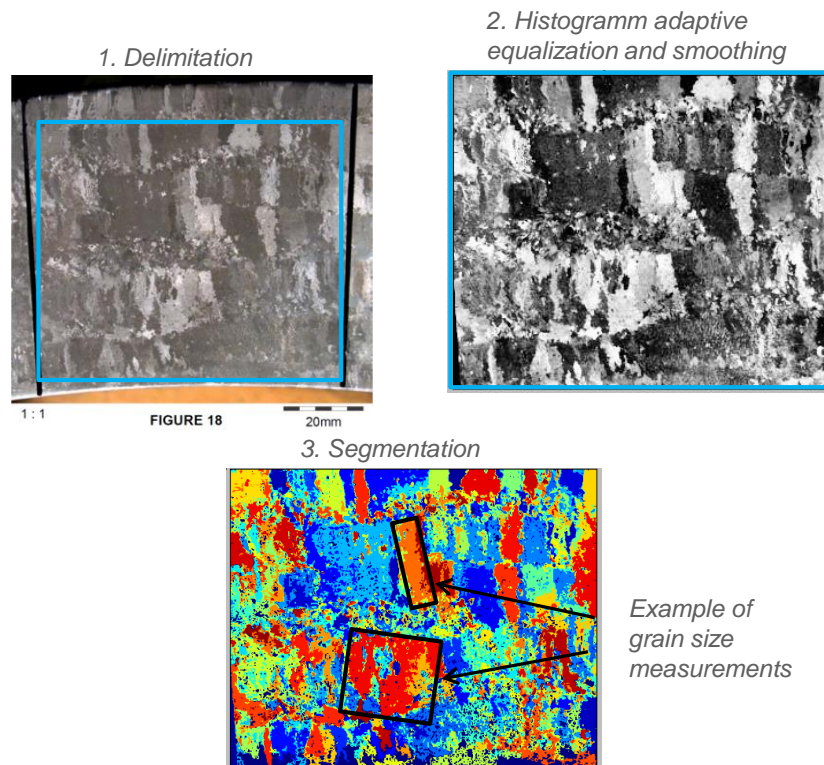


Fig. 2. Steps of image processing aimed at automatically computing the mean grain size in a given region of the component, using a macrograph.

Depending on operating conditions, the orientation of the transducer may also vary. The radial position varies namely from -1° to 1° (see blue arrow in figure 1).

Besides, parameters related to the geometry of the specimen are first the thickness of the specimen. Indeed, as explained in the former section, the thickness of the component may locally vary from 75 to 90 mm, and if the delay laws are computed for a fixed component thickness, the inspection may be degraded when inspecting a significantly different thickness. Ovalization of the pipe may also appear, but it was shown to arise with constant thickness (via profilometry of representative mock-ups), which will be taken into account by changing the radius of curvature of the specimen (without change of the wedge curvature). Lastly, another physical phenomenon occurs when an ultrasonic wave propagates in a heterogeneous structure made of coarse grains: the coherent waves undergoes amplitude and phase fluctuations. This effect will be studied later (in section 4).

3. POD Results

POD were computed with CIVA software, with 600 configurations (30 characteristic parameter values and 20 random samples of influent parameters). A cluster of computers was used to speed the process. All POD curves are computed using Hit Miss algorithm [7] with the same arbitrary detection threshold. The inspection method being new, the detection threshold is not fixed yet, and we will show in the last section how ROC curves may be used to choose the threshold appropriately. Figure 3 on the left shows the POD curve obtained when ovalization of the pipe is neglected and when the grade of stainless steel is supposed to be known (thus with small fluctuations of elastic constant).

The phased array method had been developed for defects normal to back wall. To check its ability to inspect tilted defects, the POD was computed taking into account a tilt ranging from -10° to 10° (figure 3 on the right). The $a_{90/95}$ parameter (smallest defect that the system detect with a probability of 90% with 95% confidence) is almost unchanged (11.1 mm versus 10.4 mm). The same computation was also done with defect skew ranging from -5° to 5° , without any change in the POD curve (not shown here).

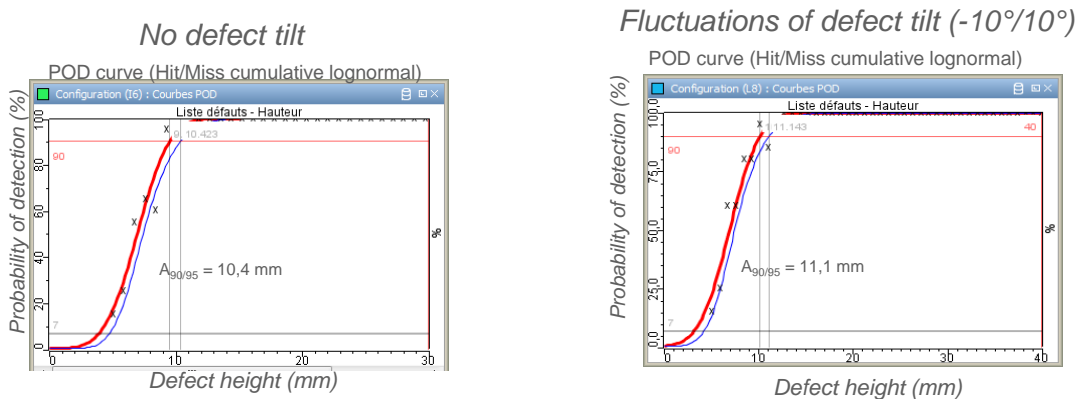


Fig. 3. Model-based POD curves computed in CIVA on notches normal to back wall (left), or with varying tilt (between -10° to 10° from normal).

The influence of outer diameter was also qualitatively studied, with computation either with fixed or with varying outer diameter (ranging from 929 mm to 945 mm), the wedge diameter being fixed. We confirmed that such small fluctuations of outer diameter have negligible impact on POD (not represented here). As for the variations of local thickness of the component, the impact on the POD is high (figure 4 on the right versus figure 4 on the left, delay laws being adapted to a 75 mm- pipe). Indeed it is important to know the precise thickness of the component under inspection to choose appropriate the delay laws.

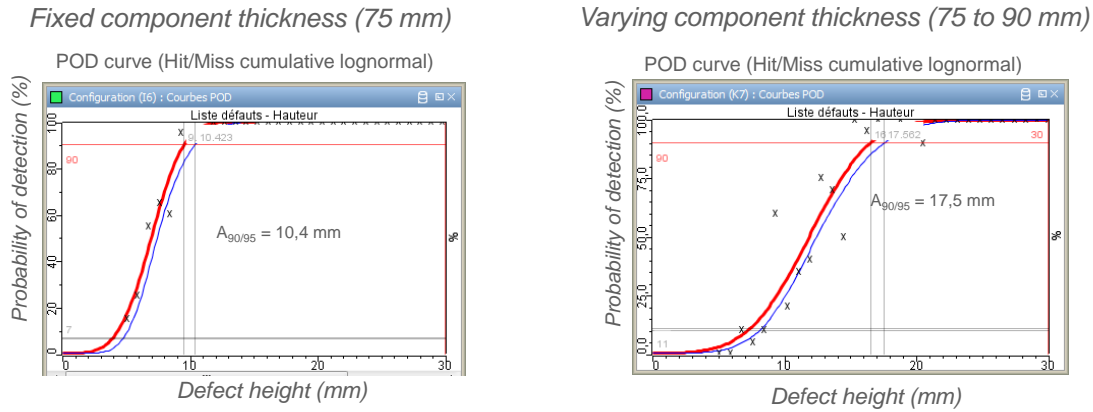


Fig. 4. Model-based POD curves computed in CIVA on notches normal to back wall when the component thickness is known and fixed (left), or when it varies from 75 to 90 mm (right). In both cases, delay laws are computed assuming the thickness is 75 mm.

Lastly, we focused on the fluctuation range of elastic constants. Figure 5 shows the POD curve computed either considering large fluctuations of c_{ij} (on the right) or limited ones (on the left). The thickness of the component was considered here to vary (still from 75 to 90 mm). The detection capability is significantly degraded when any grade of stainless steel may be encountered. Indeed, delay laws are computed using a given value of elastic constants, and are not appropriate for the inspection of a component where the elastic constants of the macro-grains are significantly different. As a conclusion, prior knowledge of stainless steel grade of current component (%Cr, %Ni) or local calibration is highly recommended.

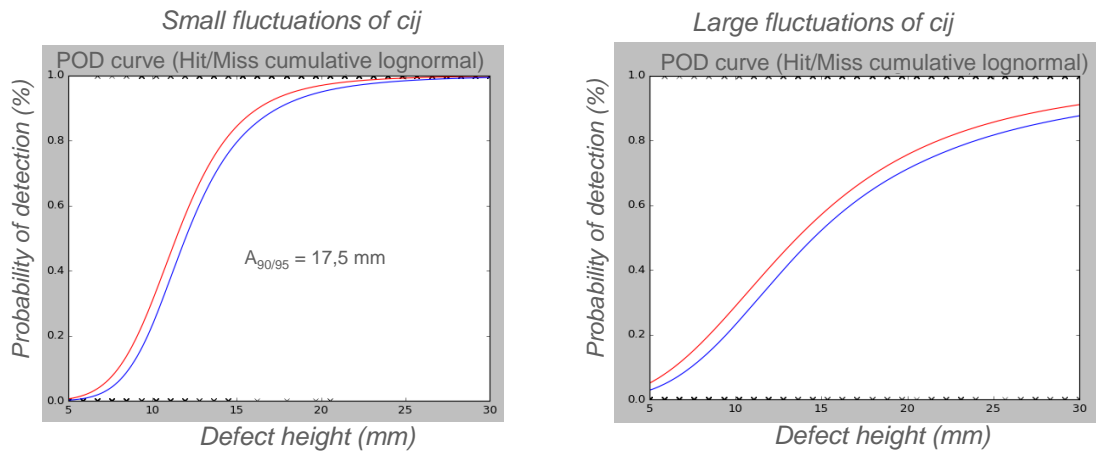


Fig. 5. Model-based POD curves computed in CIVA on notches normal to back wall, taking into account fluctuations of pipe thickness, when the stainless steel grade is known (i.e. c_{ij} vary feebly, left), or not (i.e. c_{ij} vary strongly, right).

4. Effect of Grain Size on POD

As explained in section two, when grains are large, the incident wave undergoes amplitude and phase fluctuations. This can be modelled in CIVA using Voronoi model [1]. However, the computation time is high for POD computation, so we chose here to extract this information from measurements on a representative mock-up. We assume here that the fluctuations of a breaking notch corner echo are statistically close to those of a block corner echo. In this case, we proceed as follows:

First step: We compute the defect echo amplitudes with all influent parameters but without fluctuations due to the big size of the grains.

Second step: We estimate the amplitude fluctuations of the incident wave near the bottom of the specimen due to the heterogeneous structure, using experimental data.

Third step: a random fluctuation is added to the defect echo amplitude.

Fourth step: The POD curve is computed.

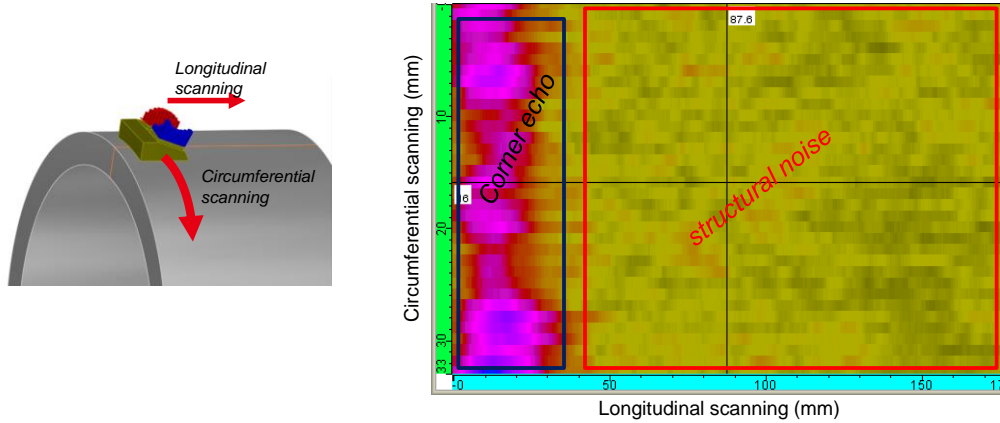


Fig. 6. Experiments on a CCSS specimen. Left: configuration, right: resulting C-scan image, displaying end-of-block corner echo (in dark blue) and back-scattered noise (red zone).

An experiment was performed on a mock-up that contains no defect (figure 6). The end-of-block corner echo is measured for each circumferential scanning position of the transducer. The fluctuations are characterized by the statistical distribution of the maxima of this echo. Before adding this fluctuations to the simulated amplitudes, they are expressed in CIVA unit using calibration (computation of end-of-block corner echo in CIVA on component with same thickness and nominal attenuation law, and comparison of mean amplitude with mean experimental block corner echo).

Figure 7 shows the POD computed without added fluctuations due to coarse grains (on the left), and the POD computed with the same simulated data to which fluctuations were added (on the right). The detection capability is clearly degraded when the effect of coarse grain is taken into account. However, as previously mentioned, the detection threshold has to be properly chosen, as it depends on the level of structural noise and impacts both probability of detection (POD) and probability of false alarms (PFA). We thus compute ROC curves to help choose the appropriate threshold.

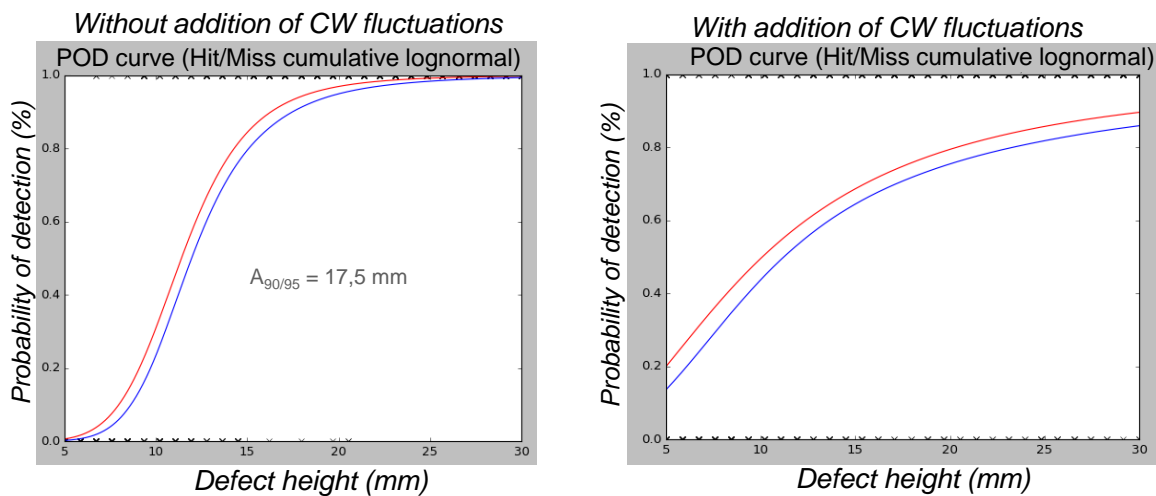


Fig. 7. POD with (on the right) or without (on the left) addition of fluctuations of coherent wave (with weak fluctuations of c_{ij} and varying component thickness).

5. Computation of Roc Curve Using Experiments and Modelling

ROC curve is the location of the points that relates the probability of false alarms (PFA) and the probability of detection (POD) for a given defect size when the detection threshold varies. The PFA is the probability for the measured amplitude to be higher than the detection threshold in the absence of a defect.

We first retrieved the probability of false alarms (PFA) from the measured backscattered signals (cf Figure 6): Away from the end-of-block, the measured signal is due to structural noise (backscattering of ultrasound by grains).

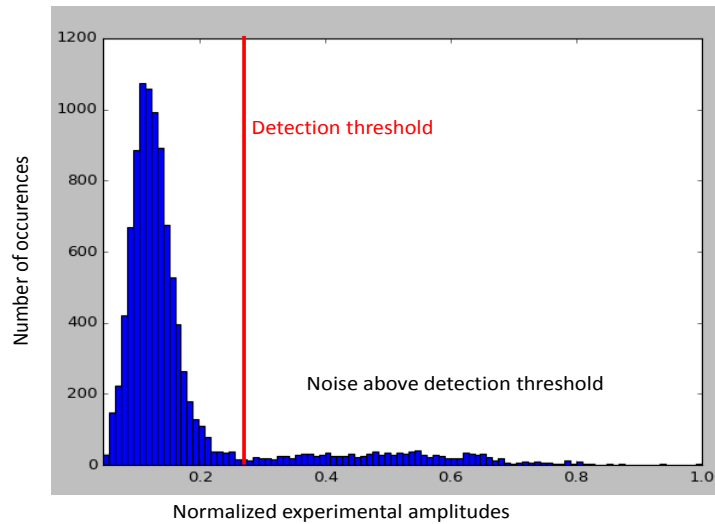


Fig. 8. Computation of PFA: histogram of backscattered noise.

The PFA is deduced from the histogram of maximum of the echo measured on each Ascan (Figure 8), in a time window in which the defect echoes are seen. PFA will namely be equal to the area right to the red line divided by the total area. On this example, the PFA is 12.6% (with equivalent detection threshold used previously for POD computation on synthetic data). The ROC curve is then simply computed for any defect size a by extraction of $POD(a)$ in CIVA POD module for any threshold. Figure 9 displays the ROC curve for a 30 mm-high defect.

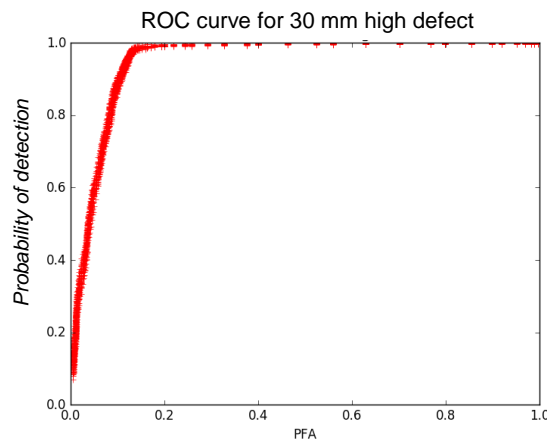


Fig. 9. ROC curve computed using experimental PFA and model-based POD curve (taking into account the fluctuations of incident wave due to grain size, and with small fluctuations of elastic constant and fixed wall thickness 75 mm).

In this study, no target value for PFA or POD was given, but given a desired maximum PFA and minimum POD, the ROC curves enables to choose the appropriate threshold.

6. Conclusion

In this paper, CIVA modelling tools were used to assess the reliability of a recent phased array inspection technique of CCSS components in nuclear power plants. Influent parameters were investigated, and macrographic examinations were used to retrieve the fluctuations of one of the influent parameters, namely the local mean grain size. The process was automatized via an image processing procedure.

POD curves were then computed with different sets of influent parameters in order to qualitatively assess the influence of these parameters. It was shown that prior knowledge of stainless steel grade and of the component thickness is important. Two approaches are possible: either the procedure could include a local measurement of the thickness under the transducer, or the inspection could be performed with a sequence of delay laws, each adapted to a given thickness and steel grade, along with appropriate post-processing of the data, in order to ensure that at least one delay law will enable the detection of the defect, in which case the knowledge of the component exact geometry is not essential any more.

A simplified approach was used to compute POD curves when taking into account all effects of coarse grain structure on ultrasound. Combining simple experiments on representative mock-ups with simulations reduces the computation time.

Structural fluctuations due to metallurgic structure of cast stainless steel are then shown to be the most influent factor degrading the reliability.

PFA were also obtained from experimental data. Lastly, ROC curves were deduced from PFA and POD for several defect sizes. It helps choose an appropriate detection threshold depending on desired inspection capabilities.

In future work, quantitative sensitivity analysis of influent parameters could be performed. It would be of particular interest to determine the range of tilt and skew of defects that can be inspected by the procedure.

The methodology could be applied to industrial cases with known target PFA and POD to determine the appropriate threshold.

References

- [1] F. Jenson, E. Iakovleva and C. Reboud, "Evaluation of POD Curves Based on Simulation Results", 7th International Conference on NDE in Relation to Structural Integrity for Nuclear and Pressurized Components, 12-15 May 2009, Yokohama, Japan.
- [2] F. Schubert, H-U. Baron, J. Menges, V. Dorval, C. Gilles-Pascaud, R. Raillon-Picot, N. Dominguez, J.-Y. Chatellier, T. Barden, "Simulation-Supported POD for Ultrasonic Testing – Recommendations from the PICASSO Project", 5th European-American Workshop on Reliability of NDE, (2013).
- [3] Nicolas Dominguez, Frederic Reverdy, and Frederic Jenson, "POD Evaluation Using Simulation: a Phased Array UT Case on a Complex Geometry Part", AIP Conf. Proc. 1581, 2031 (2014).
- [4] L. Ducouso-Ganjehi et al, « Assessment Of Reliability Of Nde For Csx And Dmw Components», 11th International Conference on NDE in Relation to Structural Integrity for Nuclear and Pressurized Components, Korea, 2015
- [5] D Gasteau et al, "Single crystal elastic constants evaluated with surface acoustic waves generated and detected by lasers within polycrystalline steel samples", J. Appl. Phys. 119, 2016
- [6] Ledbetter, "Monocrystal-Polycrystal Elastic Constants of a Stainless Steel", Phys.Stat.Sol., 1984
- [7] MIL-HDBK-1823, "Department of Defense, Handbook: nondestructive evaluation NDE system, reliability assessment", 30 april 1999.